

TRANSIENT THERMOELASTOPLASTIC STRESS ANALYSIS FOR A HOLLOW SPHERE USING THE INCREMENTAL THEORY OF PLASTICITY

H. ISHIKAWA

Department of Mechanical Engineering, Hokkaido University, Sapporo 060, Japan

(Received 28 June 1976; revised 1 December 1976)

Abstract—An analysis based on the incremental strain theory is formulated for solving the problem of an elastoplastic hollow sphere subjected to a transient temperature distribution. Thermal and material properties are assumed to be temperature dependent and the behaviour of the medium to be characterized by the Ramberg–Osgood stress-strain relation. A method of successive elastic solutions is used to obtain a numerical solution. An illustrative example shows that the effective stress is not a monotonic function of the radius, but is much dependent on the history, gradient, and distribution of the temperature in the hollow sphere. In addition, unloading in the plastically deformed region is confirmed from the detailed discussion on the distribution of strains. As a result, the analysis based on the total strain theory is not permissible for solving this kind of elastoplastic problems subjected to transient thermal loading. In the following analysis the problem is treated in a quasi-static sense and the inertia terms in the thermoelastoplastic equations are neglected.

1. INTRODUCTION

Thermoelastoplastic stress problems have attracted considerable attention over the past decade, and several investigations [1–4] on these problems have been reported. In these papers steady-state axisymmetric thermoelastoplastic problems have been treated as so called “statically determinate” without a consideration for strains and displacements. Recently, a polar symmetric transient thermal problem for a hollow sphere of the Ramberg–Osgood type material with temperature-dependent properties was solved [5] by use of the total strain theory of plasticity. However, the effective stress in a hollow sphere subjected to thermal loading seems to be not a monotonic function of the radius, but to be strongly dependent upon the history, gradient, and distribution of the temperature in the hollow sphere. Hence, the stress paths in the sphere should be very complicated, and moreover the element in the sphere might be expected to be unloaded after a certain plastic deformation. Therefore, the total strain theory of plasticity should not be applied to this kind of transient thermal problems.

This paper is concerned with a polar symmetric transient thermal problem for a hollow sphere of the Ramberg–Osgood type material [6] with temperature dependent properties by use of the incremental strain theory of plasticity. The inner boundary of the sphere is subjected to a sudden temperature rise. The numerical calculations are made using the procedure of the “method of successive elastic solutions” [7, 8].

2. THEORETICAL ANALYSIS

2.1 *Fundamental equations for stresses and strains*

We consider a hollow sphere of inner radius a and outer one b , which is initially stress free. It is subjected to a polar symmetric temperature distribution which varies with time. We assume that the initial uniform temperature of the sphere is equal to zero and that body forces and surface tractions are absent. The analysis that follows is a development of that presented by Mendelson [8].

For equilibrium and compatibility, we have the relations

$$\frac{\partial \sigma_r}{\partial r} + \frac{2}{r}(\sigma_r - \sigma_\theta) = 0 \quad (1)$$

$$\frac{\partial \epsilon_\theta}{\partial r} = \frac{1}{r}(\epsilon_r - \epsilon_\theta). \quad (2)$$

Now the total strain is the sum of an elastic component of strain, a thermal part and a plastic

component. If the temperature at a generic radius r be T at time t , then we have

$$\epsilon_{ij} = \epsilon_{ij}^E + \delta_{ij} \int_0^T \alpha \, dT + \epsilon_{ij}^P \quad (3)$$

where the subscripts i, j denote components of the appropriate tensor and α is the coefficient of thermal expansion. From eqns (3), we obtain expressions for the stress components σ_r and σ_θ for a polar symmetric transient thermal problem.

$$\begin{aligned} \sigma_r &= -\frac{E}{1-2\nu} \int \alpha \, dT + \frac{E}{(1-2\nu)(1+\nu)} [\{(1-\nu)\epsilon_r + 2\nu\epsilon_\theta\} - \{(1-\nu)\epsilon_r^P + 2\nu\epsilon_\theta^P\}] \\ \sigma_\theta &= -\frac{E}{1-2\nu} \int \alpha \, dT + \frac{E}{(1-2\nu)(1+\nu)} [\{\nu\epsilon_r + \epsilon_\theta\} - \{\nu\epsilon_r^P + \epsilon_\theta^P\}]. \end{aligned} \quad (4)$$

The coefficient of thermal expansion α , the conductivity K , the elastic modulus E , the yield stress σ_1 , the mass density γ and the specific heat C have been defined with two factors [5]. The first one is a dimensional invariant denoted by the subscript zero, and the second one is a dimensionless temperature-dependent variant denoted by an asterisk,

$$\begin{aligned} \alpha &= \alpha_0 \alpha^*(\bar{\theta}), & K &= K_0 K^*(\bar{\theta}), & E &= E_0 E^*(\bar{\theta}), \\ \sigma_1 &= \sigma_{10} \sigma_1^*(\bar{\theta}), & \gamma &= \gamma_0 \gamma^*(\bar{\theta}), & C &= C_0 C^*(\bar{\theta}) \end{aligned} \quad (5)$$

where α^* , E^* , K^* and σ_1^* are defined as follows:

$$\begin{aligned} \alpha^* &= 1 + \alpha_1 \bar{\theta}, & K^* &= 1 - K_1 \bar{\theta}, \\ E^* &= 1 - E_1 \bar{\theta}^2, & \sigma_1^* &= 1 - \sigma_{11} \bar{\theta}. \end{aligned} \quad (6)$$

We adopt the following dimensionless variables;

$$\begin{aligned} \rho &= \frac{r}{a}, & \bar{\theta} &= \frac{T}{T_0}, & \sigma_{ij}^* &= \frac{1-\nu}{E_0 \alpha_0 T_0} \sigma_{ij}, & \epsilon_{ij}^* &= \frac{1-\nu}{\alpha_0 T_0} \epsilon_{ij} \\ \tau &= \frac{K_0}{a^2 \gamma_0 C_0} t, & \bar{\sigma}^* &= \frac{1-\nu}{E_0 \alpha_0 T_0} \bar{\sigma}, & \epsilon_{ij}^{*P} &= \frac{1-\nu}{\alpha_0 T_0} \epsilon_{ij}^P \end{aligned} \quad (7)$$

where T_0 denotes any conveniently chosen reference temperature and is taken in this case to be equal to the constant inner surface temperature to which the boundary of the sphere is suddenly exposed, while the temperature at the outer surface of the sphere is zero. Taking into account the non-dimensional quantities in (7), the eqn (4) becomes

$$\begin{aligned} \sigma_r^* &= -\frac{1-\nu}{1-2\nu} E^* \int \alpha \, d\bar{\theta} + \frac{E^*}{(1-2\nu)(1+\nu)} [\{(1-\nu)\epsilon_r^* + 2\nu\epsilon_\theta^*\} - \{(1-\nu)\epsilon_r^{*P} + 2\nu\epsilon_\theta^{*P}\}], \\ \sigma_\theta^* &= -\frac{1-\nu}{1-2\nu} E^* \int \alpha^* \, d\bar{\theta} + \frac{E^*}{(1-2\nu)(1+\nu)} [\{\nu\epsilon_r^* + \epsilon_\theta^*\} - \{\nu\epsilon_r^{*P} + \epsilon_\theta^{*P}\}]. \end{aligned} \quad (8)$$

Substituting the eqn (8) into the equilibrium eqn (1) in the nondimensional form, and utilizing the compatibility eqn (2) in the non-dimensional form, we have

$$\begin{aligned} \frac{\partial}{\partial \rho} \left\{ \frac{1}{\rho^2} \frac{\partial}{\partial \rho} (\rho^3 E^* \epsilon_\theta^*) \right\} - \frac{3-5\nu}{1-\nu} \left(\epsilon_\theta^* \frac{\partial E^*}{\partial \rho} \right) - \rho \frac{\partial}{\partial \rho} \left(\epsilon_\theta^* \frac{\partial E^*}{\partial \rho} \right) &= (1+\nu) \frac{\partial}{\partial \rho} \left(E^* \int \alpha^* \, d\bar{\theta} \right) \\ &\quad - \frac{2(1-2\nu) E^* (\epsilon_r^{*P} - \epsilon_\theta^{*P})}{1-\nu} + \frac{\partial}{\partial \rho} (E^* \epsilon_r^{*P}) + \frac{2\nu}{1-\nu} \frac{\partial}{\partial \rho} (E^* \epsilon_\theta^{*P}). \end{aligned} \quad (9)$$

integrating this equation with respect to ρ and evaluating a double integral, we obtain an

expression for ϵ_{θ}^* in the form

$$E^* \epsilon_{\theta}^* = \frac{2}{3} \frac{1-2\nu}{1-\nu} \int \epsilon_{\theta}^* \frac{\partial E^*}{\partial \rho} d\rho + \frac{1+\nu}{3(1-\nu)} \frac{1}{\rho^3} \int \rho^3 \epsilon_{\theta}^* \frac{\partial E^*}{\partial \rho} d\rho + (1+\nu) \frac{1}{\rho^3} \int E^* \left(\int \alpha^* d\bar{\theta} \right) \rho^2 d\rho + \frac{2}{3} \frac{1-2\nu}{1-\nu} \int \frac{E^*(\epsilon_r^{*P} - \epsilon_{\theta}^{*P})}{\rho} d\rho + \frac{1+\nu}{3(1-\nu)} \frac{1}{\rho^3} \int E^* \rho^2 (\epsilon_r^{*P} + 2\epsilon_{\theta}^{*P}) d\rho + B_0 + \frac{B_1}{\rho^3} \quad (10)$$

where B_0 and B_1 are constants of integration which are evaluated from the boundary condition. Using the compatibility eqn (2) in the non-dimensional form and the above eqn (10), an expression for ϵ_r^* is obtained in the form

$$E^* \epsilon_r^* = \frac{2(1-2\nu)}{1-\nu} \int \epsilon_{\theta}^* \frac{\partial E^*}{\partial \rho} d\rho - 2E^* \epsilon_{\theta}^* + (1+\nu) E^* \int \alpha^* d\bar{\theta} + E^* \epsilon_r^{*P} + \frac{2\nu}{1-2\nu} E^* \epsilon_{\theta}^{*P} + \frac{2(1-2\nu)}{1-\nu} \int \frac{E^*(\epsilon_r^{*P} - \epsilon_{\theta}^{*P})}{\rho} d\rho + 3B_0. \quad (11)$$

The boundary conditions are

$$(\sigma_r^*)_{\rho=1} = 0, \quad (\alpha_r^*)_{\rho=R} = 0 \quad (12)$$

where R is equal to b/a . Substituting eqns (10) and (11) into the first eqn of (8), and expression σ_r^* is obtained in the form

$$\sigma_r^* = \frac{2}{3(1-\nu)} \int_1^{\rho} \epsilon_{\theta}^* \frac{\partial E^*}{\partial \rho} d\rho - \frac{2}{3(1-\nu)} \frac{1}{\rho^3} \int_0^{\rho} \rho^3 \epsilon_{\theta}^* \frac{\partial E^*}{\partial \rho} d\rho - \frac{2}{\rho^3} \int_1^{\rho} E^* \left(\int \alpha^* d\bar{\theta} \right) \rho^2 d\rho + \frac{2}{3(1-\nu)} \int_1^{\rho} \frac{E^*(\epsilon_r^{*P} - \epsilon_{\theta}^{*P})}{\rho} d\rho - \frac{2}{3(1-\nu)} \frac{1}{\rho^3} \int_1^{\rho} \rho^2 E^* (\epsilon_r^{*P} + 2\epsilon_{\theta}^{*P}) d\rho + \frac{B_0}{1-2\nu} - \frac{2}{1+\nu} \frac{B_1}{\rho^3}. \quad (13)$$

From eqns (12) and (13), constants B_0 and B_1 are obtained as

$$B_0 = \frac{2(1-2\nu)}{1+\nu} B_1$$

$$B_1 = \frac{R^3}{R^3-1} \frac{1+\nu}{1-\nu} \left[- \int_1^R \epsilon_{\theta}^* \frac{\partial E^*}{\partial \rho} d\rho + \frac{1}{R^3} \int_1^R \rho^3 \epsilon_{\theta}^* \frac{\partial E^*}{\partial \rho} d\rho + 3(1-\nu) \frac{1}{R^3} \int_1^R E^* \left(\int \alpha^* d\bar{\theta} \right) \rho^2 d\rho - \int_1^R \frac{E^*(\epsilon_r^{*P} - \epsilon_{\theta}^{*P})}{\rho} d\rho + \frac{1}{R^3} \int_1^R E^* \rho^2 (\epsilon_r^{*P} + 2\epsilon_{\theta}^{*P}) d\rho \right]. \quad (14)$$

Expressions for the total strains ϵ_r^* and ϵ_{θ}^* have been derived in terms of the temperature distribution $\bar{\theta}$ and the total accumulated plastic strains ϵ_r^{*P} and ϵ_{θ}^{*P} . Then the stresses σ_r^* and σ_{θ}^* can be obtained from eqns (8).

2.2 Temperature distribution

The solution of the heat conduction equation for the hollow sphere with zero initial temperature where the inner surface temperature is maintained at T_0 , constant, for $t > 0$ is shown in Refs [5] and [10] to be

$$\bar{\theta} = \frac{1}{K_1} [1 - (1 - 2K_1 \psi)^{1/2}] \quad (15)$$

$$\psi = \frac{\psi_0}{\rho} \left(\frac{R-\rho}{R-1} \right) - \frac{2\psi_0}{\pi} \frac{1}{\rho} \sum_{n=1}^{\infty} \frac{1}{n} \sin \left[\frac{n\pi(\rho-1)}{R-1} \right] \exp \left[- \left(\frac{n\pi}{R-1} \right)^2 s \right] \quad (16)$$

$$\psi_0 = 1 - \frac{K_1}{2} \quad (17)$$

where the nondimensional time s is equal to $h^*\tau$. The notation $h^* = K^*/\gamma^*C^*$ is the nondimensional factor of the diffusivity $h = h_0h^*$, and may be taken as constant[9]. Temperature distributions for the step rise in the inner surface temperature were obtained directly from eqns (15)–(17). It is convenient for the subsequent numerical calculation to get the closed form of $\partial E^*/\partial \rho$ in eqns (10), (11) and (14). Then from eqns (6), (15) and (16) we have

$$\frac{\partial E^*}{\partial \rho} = -2\bar{\theta}E_1 \frac{\partial \bar{\theta}}{\partial \rho} = -2\bar{\theta}E_1(1 - 2K_1\psi)^{-1/2} \frac{\partial \psi}{\partial \rho} = 2\bar{\theta}E_1(1 - 2K_1\psi)^{-1/2} \times \left[\frac{\psi}{\rho} + \frac{\psi_0}{\rho} \frac{1}{R-1} \left\{ 1 + 2 \sum_1^\infty \cos \left[\frac{n\pi(\rho-1)}{R-1} \right] \exp \left[- \left(\frac{n\pi}{R-1} \right)^2 s \right] \right\} \right]. \tag{18}$$

2.3 The total accumulated plastic strains

Using the von Mises yield criterion and associated flow rule as expressed in the familiar Prandtl–Reuss equations, the total accumulated plastic strains can be determined theoretically from the integration of the infinitesimal plastic strain increments occurring at any instant over an actual loading path. However, in this paper, the total accumulated plastic strains are obtained by summation of the increments of plastic strains that occur during small intervals of time, each time interval corresponding to a particular change in temperature. After some loading path, let the total plastic strains be ϵ_{ij}^{*P} . Let the plastic strain increments $\Delta \epsilon_{ij}^{*P}$ be produced in the small interval Δt . Then total strains

$$\epsilon_{ij}^* = \epsilon_{ij}^{*E} + \epsilon_{ij}^{*P} + \delta_{ij} \int \alpha^* d\bar{\theta} + \Delta \epsilon_{ij}^{*P}. \tag{19}$$

“Modified total strains” are now defined[8]

$$\epsilon_{ij}^{*'} \equiv \epsilon_{ij}^* - \epsilon_{ij}^{*P}. \tag{20}$$

The deviatoric components are

$$e_{ij}^{*'} = \epsilon_{ij}^{*'} - \frac{1}{3} \epsilon_{ii}^{*'} = e_{ij}^{*E} + \Delta \epsilon_{ij}^{*P}. \tag{21}$$

The Prandtl–Reuss equations, with the plastic strain increments expressed simply in terms of strain, are represented as follows[8].

$$\Delta \epsilon_{ij}^{*P} = \frac{\Delta \epsilon_P^*}{\epsilon_{ei}^*} e_{ij}^{*'} \tag{22}$$

where an “equivalent modified total strain” ϵ_{ei}^* is defined as

$$\epsilon_{ei}^* = \sqrt{\left[\left(\frac{2}{3} e_{ij}^{*'} e_{ij}^{*'} \right) \right]}. \tag{23}$$

From eqns (21) and (22) we have in this problem

$$\Delta \epsilon_r^{*P} = \frac{2}{3} \frac{\Delta \epsilon_P^*}{\epsilon_{ei}^*} (\epsilon_r^{*'} - \epsilon_\theta^{*'}), \quad \Delta \epsilon_\theta^{*P} = \frac{1}{3} \frac{\Delta \epsilon_P^*}{\epsilon_{ei}^*} (\epsilon_\theta^{*'} - \epsilon_r^{*'}) \tag{24}$$

then ϵ_{ei}^* is represented as follows

$$\epsilon_{ei}^* = \frac{2}{3} |\epsilon_r^{*'} - \epsilon_\theta^{*'}|. \tag{25}$$

The quantity ϵ_{ei}^* has no physical interpretation but through the simple tension stress-strain curve a relation can be obtained between ϵ_{ei}^* , the equivalent plastic strain increment $\Delta \epsilon_P^*$ and

equivalent stress $\bar{\sigma}_{i-1}^*$ [8].

$$\Delta \epsilon_p^* = \frac{\epsilon_{\alpha i}^* - \frac{2}{3} [(1 + \nu)/E^*] \bar{\sigma}_{i-1}^*}{1 + \frac{2}{3} [(1 + \nu)/E^*] \left(\frac{d\bar{\sigma}^*}{d\epsilon_p^*} \right)_{i-1}} \tag{26}$$

In the polarly symmetric case under consideration, the equivalent stress becomes

$$\bar{\sigma}^* = |\sigma_r^* - \sigma_\theta^*| \tag{27}$$

In equation (26), $(d\bar{\sigma}^*/d\epsilon_p^*)_{i-1}$ is the value of $d\bar{\sigma}^*/d\epsilon_p^*$ up to the end of the $(i - 1)$ th interval. In this paper, the following Ramberg–Osgood type stress-strain relation will be employed with the uniaxial stress σ_i and strain ϵ_i [6].

$$\epsilon_i = \frac{\sigma_i}{E} \left[1 + \frac{3}{7} \left(\frac{\sigma_i}{\sigma_1} \right)^{m-1} \right] \tag{28}$$

From above equation the relation between the equivalent stress and plastic strain are as follows

$$\epsilon_p = \frac{3}{7} \frac{\bar{\sigma}}{E} \left(\frac{\bar{\sigma}}{\sigma_1} \right)^{m-1} \tag{29}$$

Taking into account eqn (5), the nondimensional representation of eqn (29) is

$$\epsilon_p^* = \frac{3}{7} \frac{\bar{\sigma}^*}{E^*} \lambda^{m-1} \left(\frac{\bar{\sigma}^*}{\sigma_1^*} \right)^{m-1} \tag{30}$$

where $\lambda = E_0 \alpha_0 T_0 / (1 - \nu) \sigma_{10}$ is a quantity called hereafter the loading parameter. Then, from eqn (30)

$$\frac{d\bar{\sigma}^*}{d\epsilon_p^*} = \frac{7}{3m} \frac{E^*}{\lambda^{m-1}} \left(\frac{\sigma_1^*}{\bar{\sigma}^*} \right)^{m-1} \tag{31}$$

Substituting the above equation into (26), we finally have

$$\Delta \epsilon_p^* = \frac{\epsilon_{\alpha i}^* - \frac{2}{3} [(1 + \nu)/E^*] \bar{\sigma}_{i-1}^*}{1 + \frac{14}{9} \left(\frac{1 + \nu}{m} \right) \left(\frac{1}{\lambda} \right)^{m-1} \left(\frac{\sigma_1^*}{\bar{\sigma}^*} \right)_{i-1}^{m-1}} \tag{32}$$

Consequently the components of plastic strain increment can be obtained from eqns (20), (24), (25) and (32).

3. THE RESULTS OF NUMERICAL CALCULATION

3.1 Thermal and material properties

For the thermal and material properties, we assume both for $m = 9$ and 19 in eqn (28) the following figures from D. Ghosh Dastidar and P. Ghosh [5]:

$$\begin{aligned} \alpha_0 &= 6.5 \times 10^{-6} \text{ } ^\circ\text{F}^{-1}, & K_0 &= 2.23 \text{ Btu/in hr } ^\circ\text{F} \\ E_0 &= 30 \times 10^6 \text{ psi}, & \sigma_{10} &= 48.75 \times 10^3 \text{ psi} \end{aligned} \tag{33}$$

$$\begin{aligned} \alpha_1 &= 0.138462\lambda, & K_1 &= 0.033\lambda \\ E_1 &= 0.00779135\lambda^2, & \sigma_{11} &= 0.07142857\lambda. \end{aligned} \tag{34}$$

The stress-strain curves for $m = 9$ and 19 in eqn (28) correspond to those of steel with the addition of molybdenum and with the addition of molybdenum and chromium, respectively. Poisson's ratio ν is assumed to be unaffected by temperature and to be equal to $\nu = 0.4$. Then, it is easily shown that $T_0 = 150\lambda$ with eqns (33). Now introducing the nondimensional representation

$$e_t = \frac{E_0}{\sigma_{10}} \epsilon_t \quad \text{and} \quad s_t = \frac{\sigma_t}{\sigma_{10}} \quad (35)$$

eqn (28) becomes

$$E^* e_t = s_t \left[1 + \frac{3}{7} \left(\frac{s_t}{\sigma_t^*} \right)^{m-1} \right]. \quad (36)$$

Figure 1 shows the stress-strain relation (36) in temperature fields with the value of loading parameter $\lambda = 6$, considering eqns (6) and (34). It is clear that from eqns (6) and (34) the results at $\bar{\theta} = 0$ in Fig. 1 correspond to the stress strain relation at the outer surface of the sphere and those at $\bar{\theta} = 1$, i.e. $T_0 = 900^\circ\text{F}$, to that at the inner surface of the sphere. Then, the stress strain relation at any points of sphere where the temperature could be decided by eqns (15)–(17) must be determined with eqn (36) and maybe lie between $\bar{\theta} = 0$ and 1 . In Fig. 1 the stress strain relation at $\bar{\theta} = 0.5$, i.e. $T = 450^\circ\text{F}$, are shown as an illustrative example. With increase of the exponent m in the Ramberg–Osgood stress strain relation, the behaviour of material is nearly similar to that defined as an elastic perfectly-plastic material, and only the result for $m = 101$ at $\bar{\theta} = 0$ are shown also in Fig. 1.

3.2 The procedure of the calculation

In the numerical calculations, the hollow sphere is divided into 80 radial increments. The period during which the thermal load is applied is divided into 35 time increments. The computation of the plastic strain increments that occur during a particular time increment (Δs) is carried out as follows.

Computation begins with the determination of the temperature distribution at time $(s + \Delta s)$ with eqns (15)–(17). An iterative procedure is used to determine the total strains at each radial station. From eqns (10), (11), (14) and (18), a first approximation to the total strains is obtained by setting the plastic strain increments to zero and the total accumulated plastic strains (ϵ_t^{*P} , ϵ_θ^{*P}) to the value of these up to the end of the $(i - 1)$ th interval at time s . On that occasion, the values of ϵ_t^* in a right hand side of eqns (10) and (14) should be set at first to the

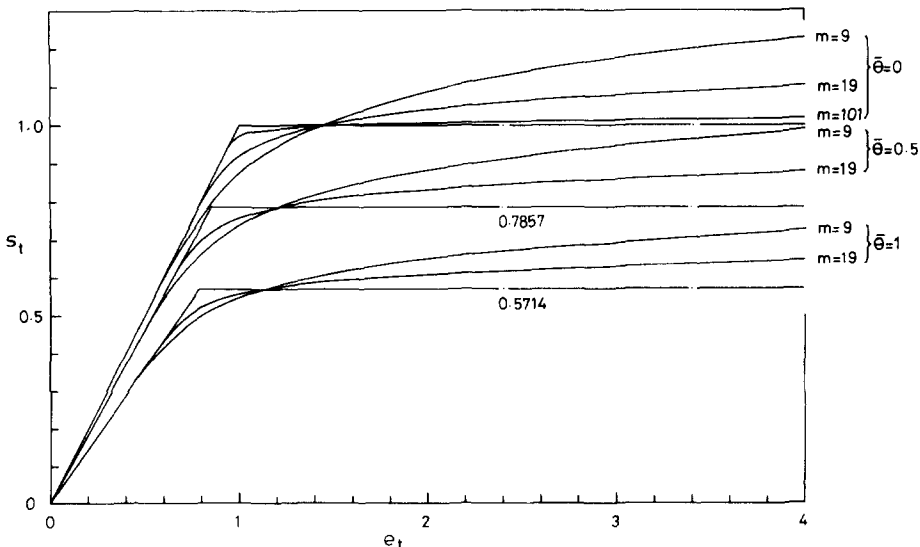


Fig. 1. Ramberg–Osgood stress and strain relation for $\lambda = 6$.

values of these at time s . The new estimated values of ϵ_{θ}^* are then used to obtain a better approximation. After convergence, the strain ϵ_r^* can be computed from eqn (11). The "equivalent modified total strain" ϵ_{et}^* are obtained from eqns (20) and (25). At each radial station the value of ϵ_{et}^* is compared with $\frac{2}{3}[(1-\nu)/E^*]\bar{\sigma}_{i-1}^*$ (see eqn (32)). If $\epsilon_{et}^* < \frac{2}{3}[(1+\nu)/E^*]\bar{\sigma}_{i-1}^*$, then that particular radial station is situated in an elastic region, and correspondingly, $\Delta\epsilon_{\theta}^*$ is set to zero. On the other hand, if $\epsilon_{et}^* > \frac{2}{3}[(1+\nu)/E^*]\bar{\sigma}_{i-1}^*$, then the particular radial station is situated in a plastic zone, and the appropriate value of the "equivalent plastic strain increment" $\Delta\epsilon_{\theta}^{*P}$ is evaluated from eqn (32). First approximation are then calculated for $\Delta\epsilon_r^{*P}$ and $\Delta\epsilon_{\theta}^{*P}$ from the modified Prandtl-Reuss relations (24). These values are then used to obtain a better approximation for the total strains ϵ_r^* and ϵ_{θ}^* . This process should be repeated as many times as is necessary to obtain the desired degree of convergence. After convergence, the stresses σ_r^* and σ_{θ}^* can be computed from eqns (8). The accumulated plastic strains at time $(s + \Delta s)$ are now updated so as to include the plastic strain increments which have been determined by this iterative procedure. Computation then proceeds for the next increment of time.

Figure 2 shows the variation of temperature $\bar{\theta}$ with respect to $1/\rho$, i.e. a/r for different values of time s for $\lambda = 6$ and $m = 9$ when $R = 5$ with the solid lines for a sensitive material. The results for an insensitive material are also represented in Fig. 2 with the alternate long and short dash line only at the steady state, i.e. $s = 50$, to avoid complexity of the figure. Fig. 3 shows the variation of σ_r^* and σ_{θ}^* with respect to $1/\rho$ both for a sensitive and an insensitive material at times $s = 0.5$ and 4 for $\lambda = 6$ and $m = 9$ when $R = 5$. This figure shows that the elastic plastic boundary of a sensitive material which is recognized in this figure as at the point of inflexion in the distribution for σ_{θ}^* is developed closer to the outer surface than that of an insensitive one at each time s . Besides for an insensitive material, it is clear from this figure that unloading may arise near the inner surface with increase of time s . At the same radial station in the plastically deformed region, the stresses for a sensitive material are always smaller than those for an insensitive one as shown in the figure. Figure 4 shows the variation of $E\epsilon_r^P/\lambda\sigma_{10}$ and $E\epsilon_{\theta}^P/\lambda\sigma_{10}$ with respect to $1/\rho$ both for a sensitive and an insensitive material at times $s = 0.5$ and 4, similarly as in Fig. 3. The radial stations where the plastic strains $E\epsilon_r^P/\lambda\sigma_{10}$ and $E\epsilon_{\theta}^P/\lambda\sigma_{10}$ become zero are considered to be the elastic plastic boundaries and correspond to the stations of the points of inflexion in the distributions of the circumferential stress σ_{θ}^* in Fig. 3. From a detained discussion on the total strains and the total accumulated plastic strains, we can recognize the occurrence of unloading near the inner surface of the sphere. Namely, at that occasion, the total strains clearly decrease, while the total accumulated plastic strains hold constant during time increment Δs . Though this occurrence of unloading will be examined later in detail with variation of the effective stress, it should be predicted that this result should be different from that in [5] obtained by use of the total strain theory of plasticity. In Fig. 5 both results obtained by the author, and D. Ghosh Dastidar and P. Ghosh[5] are represented by

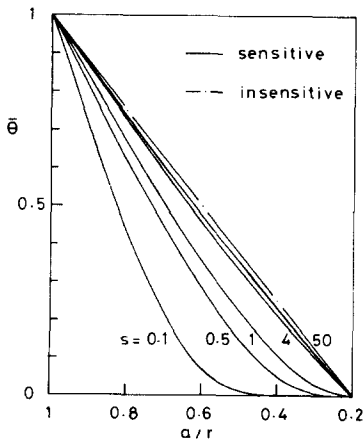


Fig. 2.

Fig. 2. Temperature distributions for various times s for $\lambda = 6$, $m = 9$ when $b/a = 5$.

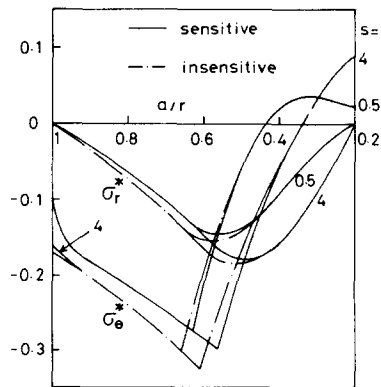


Fig. 3.

Fig. 3. Stress distributions both for a sensitive and an insensitive material for $\lambda = 6$, $m = 9$ when $b/a = 5$.

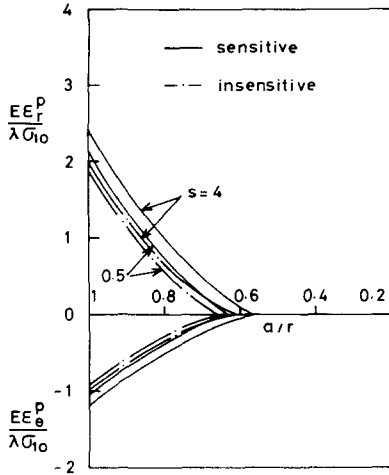


Fig. 4.

Fig. 4. Plastic strain distributions both for a sensitive and an insensitive material for $\lambda = 6$, $m = 9$ when $b/a = 5$.

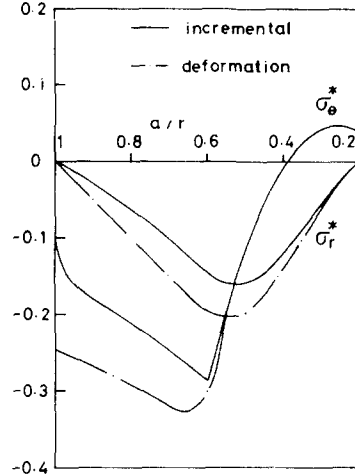


Fig. 5.

Fig. 5. Comparison with the results by the total strain theory for $\lambda = 6$, $m = 9$ when $b/a = 5$ at $s = 1$.

solid lines and the alternate long and short dash lines, respectively, when $R = 5$. The discrepancy between these two results is recognized distinctly in the plastically deformed region.

Without consideration for strains and displacements, the steady state thermoelastoplastic problem for this hollow sphere of an elastic perfectly plastic material is solved by use of only an equilibrium equation and a yield criterion, as so called "statically determinate". On the other hand, for large values of the exponent m in the Ramberg-Osgood relation, the shape of the curve approaches that of the elastic perfectly-plastic material, as previously mentioned. So the result calculated with large value of the exponent $m = 101$ (see Fig. 1) is compared with that in [11] for the elastic perfectly-plastic material.

The solid lines in Fig. 6 show the variation of σ_r^* and σ_e^* obtained by the author with respect to $1/\rho$ for the steady state, i.e. at time $s = 50$, for $\lambda = 6$ and $m = 101$ when $R = 5$. Then, the radial station of the elastic plastic boundary R_c should be set to 1.65 from that of the point of inflexion in the distribution of the circumferential stress σ_e^* where the total accumulated plastic strains become zero, as previously mentioned. The results for the elastic perfectly-plastic material treated as "statically determinate" for $\lambda = 6$ and $R_c = 1.65$ are also shown in Fig. 6 by the alternate long and short dash lines when $R = 5$. With the exception of the neighbourhood of

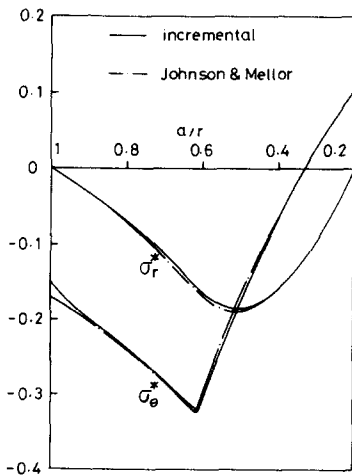


Fig. 6.

Fig. 6. Comparison with the results for an elasto perfectly-plastic material for $\lambda = 6$, $m = 101$ when $b/a = 5$ at $s = 50$.

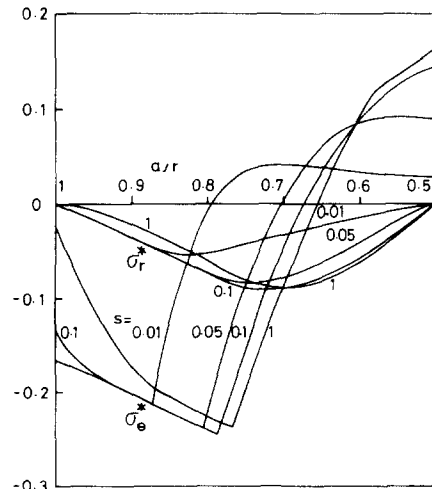


Fig. 7.

Fig. 7. Stress distributions for an insensitive material for $\lambda = 6$, $m = 19$ when $b/a = 2$.

the inner surface, where unloading is recognized in the author's results, both results are in good agreement with each other.

Figure 7 shows the variation of σ_r^* and σ_θ^* with respect to $1/\rho$ for an insensitive material at times $s = 0.01, 0.05, 0.1$ and 1 for $\lambda = 6$ and $m = 19$ when $R = 2$. Because of the smaller thickness of the hollow sphere, the steady state in the temperature distribution can be obtained at a smaller time $s = 1$ than when $R = 5$. Though the stress σ_r^* in the plastically deformed region maintains the constant value at time $s = 0.01$ and 0.05 , unloading occurs near the inner surface of the hollow sphere at time $s = 0.1$. Then the variation of σ_r^* at time $s = 1$ becomes much different from that at other time s . Namely, the second point of inflexion can be shown clearly at the neighbourhood of the outer surface.

Figure 8 shows the variation of $\bar{\sigma}$ with respect to $1/\rho$ for an insensitive material at times $s = 0.04, 0.1, 0.2$ and 1 for $\lambda = 6$ and $m = 19$ when $R = 2$. The quantity $\bar{\sigma}$ is the nondimensional equivalent stress which is defined as follows:

$$\bar{\sigma} = \frac{\bar{\sigma}}{\sigma_{10}} = \lambda \bar{\sigma}^* \tag{37}$$

Since $\sigma_r^* = 1 - \sigma_{11}\bar{\theta} = \sigma_r/\sigma_{10}$ from eqns (5) and (6), the radial station where $\bar{\sigma} \geq \sigma_r^*$ is the region under yielding. On the other hand, the radial station where $\bar{\sigma} < \sigma_r^*$ is either the region on elastic loading without the plastic strains or the region on unloading with the plastic strains. For an insensitive material, the radial station where $\bar{\sigma} \geq \sigma_r^* = 1$ is the region under yielding. Then, from Fig. 8 the neighbourhood of inner surface is the plastic region under yielding until time $s = 0.04$. At large time $s = 0.1$ the hollow sphere is divided into three regions in the radial direction, that is, from the inner surface to the outer one, the plastic region under unloading, the plastic region under yielding and the elastic region under loading where it should be predicted by the large value of $\bar{\sigma}$ to start to yield in short time, and at time $s = 0.2$, the yielding begins abruptly in this third region. The result at time $s = 1$ in Fig. 8 shows the steady state solution. The radial station of the second point of inflexion in Fig. 7 corresponds to the station of the second elastic plastic boundary, as might be expected.

With same situation as in Fig. 8, Fig. 9 shows the variation of $E\epsilon_r^P/\lambda\sigma_{10}$ with respect to $1/\rho$. Then, from eqn (24), we can estimate the value of $E\epsilon_\theta^P/\lambda\sigma_{10}$ to be equal to $(-1/2)(E\epsilon_r^P/\lambda\sigma_{10})$. The variation of $E\epsilon_r^P/\lambda\sigma_{10}$ is not recognized at the neighbourhood of the inner surface, where the plastic strain increments are not accompanied with the time increments. Even though

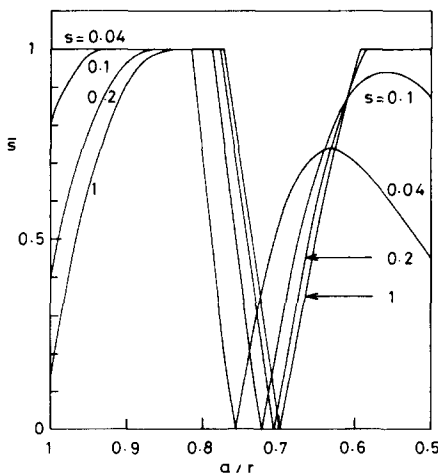


Fig. 8.

Fig. 8. Equivalent stress distributions for an insensitive material for $\lambda = 6, m = 19$ when $b/a = 2$.

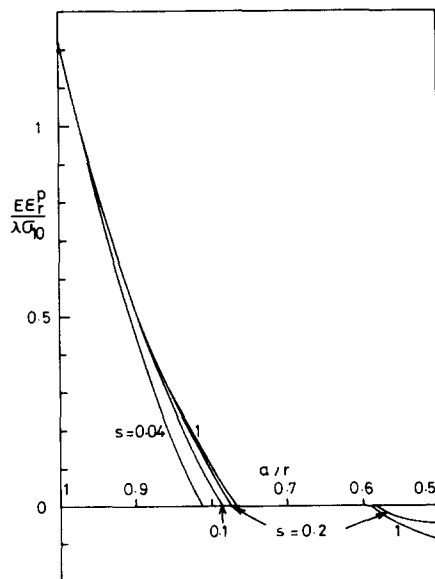


Fig. 9.

Fig. 9. Plastic strains distributions for an insensitive material for $\lambda = 6, m = 19$ when $b/a = 2$.

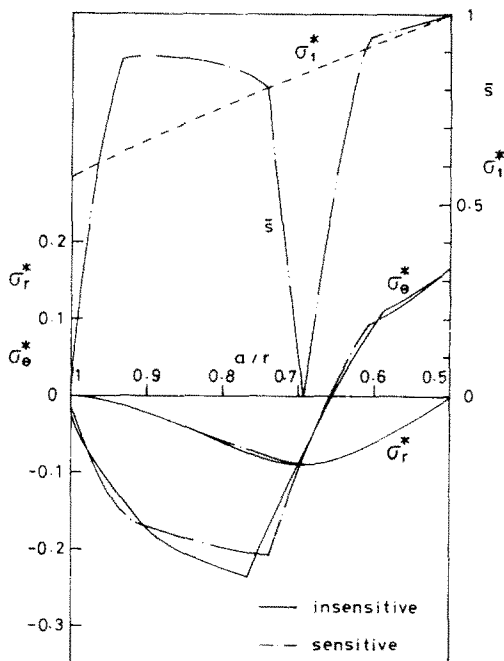


Fig. 10. Stress distributions both for a sensitive and an insensitive material for $\lambda = 6$, $m = 19$ when $b/a = 2$.

without the special representation of figure, the total strains in this region are decreased. Namely as $\bar{s} < \sigma_1^* = 1$ from Fig. 8, this plastic region is recognized to be under unloading. The second plastically deformed region is shown in Fig. 8 at the neighbourhood of the outer surface of hollow sphere, and the radial stations of $E\epsilon_r^p/\lambda\sigma_{10} = 0$ correspond to those of the elastic plastic boundaries shown in Figs. 7 and 8. Johnson and Mellor[11] in their paper pointed out that for the elastic perfectly-plastic material for $R = 2$, a second plastic zone starts to develop at a temperature of 360°F.

Figure 10 shows the variation of σ_r^* and σ_θ^* with respect to $1/\rho$ both for a sensitive and an insensitive material at time $s = 1$ for $\lambda = 6$ and $m = 19$ when $R = 2$. Also in this figure, the variation of \bar{s} and σ_1^* with respect to $1/\rho$ for a sensitive material is shown. As previously mentioned, the region where $\bar{s} \geq \sigma_1^*$ is defined as to be under plastic yielding. While the region where $\bar{s} < \sigma_1^*$ is defined as to be under elastic loading except the neighbourhood of the inner surface where is now to be under unloading after yielding. Moreover, the elastic plastic boundaries for a sensitive material are developed closer to the interior of hollow sphere from both inner and outer surfaces.

4. CONCLUSION

By use of an incremental strain theory of plasticity, the thermoelastoplastic solution of a hollow sphere of the Ramberg-Osgood type material with temperature dependent properties is presented. From the numerical calculation based on the "method of successive elastic solutions", the following conclusions are obtained;

(1) At the neighbourhood of the inner surface, unloading in the first plastic zone occurs with time both for $R = 5$ and 2, and besides the second plastic zone starts to develop at the neighbourhood of the outer surface for $R = 2$.

(2) The discrepancy between the results obtained in this paper and by the total strain theory of plasticity is recognized distinctly in the plastically deformed region. This suggests that the application of the total strain theory of plasticity to this kind of transient thermoelastoplastic problem is not suitable[12], because of unloading.

(3) The steady state solution obtained as "statically determinate" for an elastic perfectly-plastic material corresponds to a special situation in this solution presented, in which case both results are in good agreement.

(4) The values of stresses for a sensitive material are usually smaller than those for an insensitive one in the plastically deformed region, and the elastic plastic boundaries of a

sensitive material develop closer to the interior of the hollow sphere than those of an insensitive one.

Acknowledgements—The author wishes to thank the Hokkaido University Computing Center for the use of their computer FACOM 230-75.

REFERENCES

1. J. H. Weiner, *J. Appl. Mech.* **23**, 395 (1956).
2. C. Hwang, *J. Appl. Mech.* **27**, 629 (1960).
3. H. G. Landan and E. E. Zwicky, *J. Appl. Mech.* **27**, 491 (1960).
4. D. R. Band, *J. Mech. Phys. of Solid* **4**, 209 (1956).
5. D. Ghosh Dastidar and P. Ghosh, *Int. J. Mech. Sci.* **16**, 359 (1974).
6. W. Ramberg and W. R. Osgood, *NACA TN* 902 (1943).
7. D. G. Owen, *Int. J. Mech. Sci.* **16**, 313 (1974).
8. A. Mendelson, *Plasticity, Theory and Application*, p. 164. Macmillan, New York (1968).
9. R. Trostel, *Ing-Arch.* **26**, 416 (1958).
10. H. S. Carslaw and J. C. Jaeger, *Conduction of Heat in Solids*, 6th Edn. Clarendon Press, Oxford (1959).
11. W. Johnson and P. R. Mellor, *Engineering Plasticity*, pp. 202–219. Van Nostrand Reinhold, New York (1973).
12. R. Hill, *The Mathematical Theory of Plasticity*, p. 47. Clarendon Press, Oxford (1950).